

THERMODYNAMIC CHARACTERIZATION OF CARBON BLACK-FILLED RUBBERS

*V. P. Privalko, V. P. Azarenkov, A. V. Baibak and Y. G. Yanovsky**

Institute of Macromolecular Chemistry, National Academy of Sciences of Ukraine,
253160 Kiev, Ukraine

*Institute of Applied Mechanics, Russian Academy of Sciences, 117334 Moscow, Russia

(Received May 5, 1995)

Abstract

Unfilled and carbon black-filled samples of synthetic isoprene- and butadiene-methylstyrene-based rubbers were characterized by precise heat capacity measurements in the temperature interval 4.2–300 K. Both unfilled samples proved to behave in an essentially fracton-like way in the temperature interval 6–30 K. The excess thermodynamic quantities derived from the smoothed data suggested that the thermodynamic state of the elastomeric phase in the filled rubbers was intrinsically unstable.

Keywords: excess thermodynamic quantities, filled rubbers, fracton-like vibration regime, heat capacity, thermodynamic stability

Introduction

The incorporation of high-modulus, disperse solid fillers into a low-modulus, continuous elastomeric phase has long been (and still is) an obvious pragmatic approach to improvement of the mechanical performance of rubbers. In the majority of documented cases (e.g. [1–3]), either a large (in the case of ‘reinforcing’ fillers) or a small (in the case of ‘inert’ fillers) ‘overshoot’ of the experimental elasticity moduli above the estimates based on various hydrodynamic theories was almost invariably observed, as if the apparent volume content of the disperse phase, φ^* , exceeded its nominal content, φ . A seemingly reasonable explanation of this empirical finding was that a ‘bound’ rubber (BR) structurally different from the remainder of a continuous elastomeric matrix formed concentric shells of reduced thickness $\Delta r/r = (\varphi^*/\varphi)^{1/3} - 1$ around the filler particles of size $2r$ (assuming, for simplicity, the spherical shape of the latter). In spite of many attempts to evaluate the structure and ‘partial’ properties of BR (e.g. [4–6]), its thermodynamic stability has so far not been characterized.

It is therefore the purpose of the present communication to provide the first direct experimental data on the thermodynamic state of BR in carbon black-filled rubbers.

Experimental

Flat specimens (thickness 1–3 mm) of synthetic isoprene rubber SKI-3 and synthetic butadiene-dimethylstyrene rubber SKMS-30 filled with furnace carbon black TU P-234 (specific surface area about $240 \text{ m}^2 \text{ g}^{-1}$) were prepared by hot-pressing at 350–370 K. Sample codings and compositions are shown in Table 1.

Table 1 Sample coding and composition (in parts by weight)

| Ingredient | Sample coding | | | | |
|-------------------|---------------|------|------|------|------|
| | M340 | M342 | M344 | D200 | D240 |
| SKI-3 | 200 | 200 | 200 | – | – |
| SKMS-30 | – | – | – | 200 | 200 |
| Stearic acid | 2 | 2 | 2 | 4 | 4 |
| Altax | 1.2 | 1.2 | 1.2 | – | – |
| Diphenylguanidine | 6 | 6 | 6 | – | – |
| Zinc oxide | 10 | 10 | 10 | 10 | 10 |
| Carbon black | 0 | 40 | 80 | 0 | 80 |
| Sulfur | 2 | 2 | 2 | 4 | 4 |
| Sulfeneamide | – | – | – | 3 | 3 |

The heat capacity C_p in the temperature interval 4.2–300 K was measured in steps of 0.2–0.6 K in the interval 4.2–50 K, 0.6–1.5 K in the interval 50–150 K and 1.5–5 K at higher temperatures, with the aid of an automated adiabatic calorimeter [7]; the estimated maximum errors in the indicated temperature intervals did not exceed 2%, 1% and 0.5%, respectively.

Results and discussion

Heat capacity in the solid state

The raw values of the heat capacity C_p for all studied samples in the entire temperature interval of the solid (i.e. glassy) state below about 200 K varied smoothly with temperature T (Fig. 1). As can be seen from the $\log C_p$ vs. $\log T$ plots (Fig. 2), the experimental data for both unfilled samples M-340 and D-200 below 20 K may be reasonably well fitted to the Stockmayer-Hecht (SH) model [8], assuming $T^* = 370$ K for the characteristic temperature, $\nu^* = 255 \text{ cm}^{-1}$

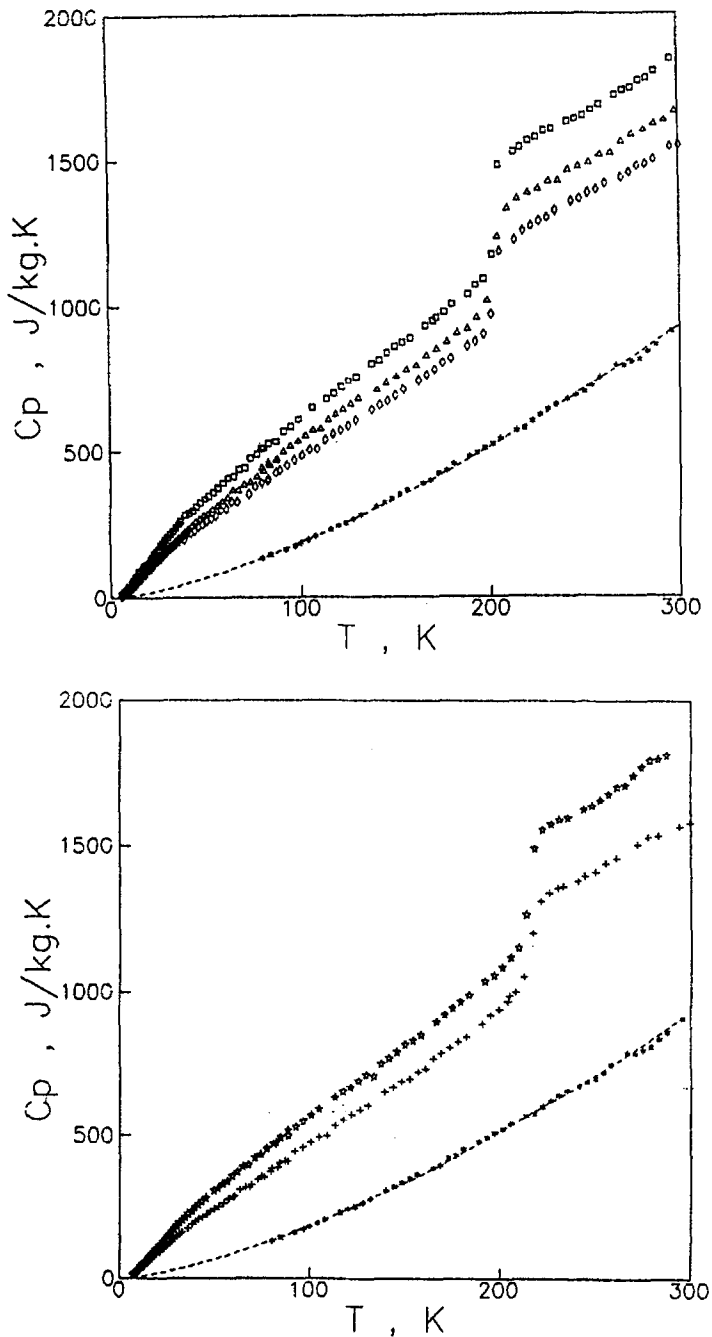


Fig. 1 Temperature dependence of the raw heat capacity of M-340 (squares), M-342 (triangles), M-344 (diamonds), D-200 (stars), D-240 (crosses) and carbon black (asterisks)

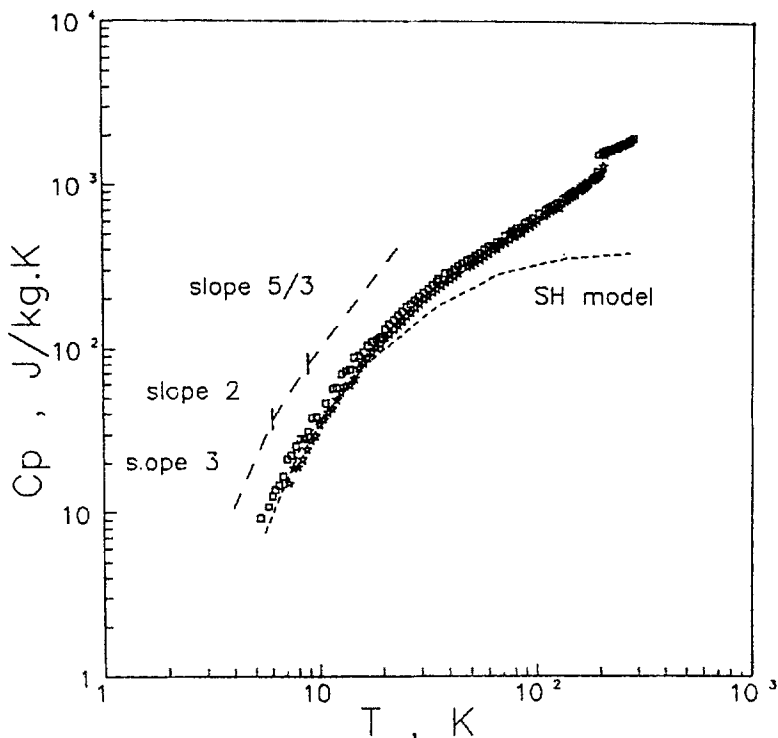


Fig. 2 $\text{Log}C_p$ vs. $\text{log}T$ plots for M-340 and D-200

for the characteristic frequency of vibrations, and $m^* = 40 \text{ g mol}^{-1}$ for the effective mass of the chain vibrating unit (regarding the observed variation in these parameters with the polymer nature [9] as unessential). It is pertinent to remark here, however, that the SH model, in a strict sense, was developed for polymer crystals; therefore, one should look for a different approach explicitly accounting for a disordered structure of the studied rubbers in the glassy state.

There is experimental evidence suggesting that polymer glasses behave essentially fractal-like in the frequency interval from about $\omega' = 20$ to $\omega'' = 80 \text{ cm}^{-1}$ [10–13]; therefore, one should expect a cross-over of the vibration density of the states, $\rho(\omega) \sim \omega^{d-1}$ (where $d = D/a$, D is the mass fractal dimensionality and a is the low-frequency scaling exponent), to the fracton-like vibration regime [14, 15] in the temperature interval from $T' = h\omega'/k = 5 \text{ K}$ to $T'' = h\omega''/k = 20 \text{ K}$. In fact, analysis of the experimental $C_p \sim \int \rho(\omega) d\omega \sim T^d$ data for several polymers in the indicated temperature interval [16] revealed a surprisingly good agreement of the experimental exponents d with the theoretical $d = D = 2$ and $5/3$ (below and above 10 K, respectively) predicted on the assumption that $a = 1$ (i.e. the high conductivity limit). The raw values of C_p for both unfilled rubbers apparently exhibit similar behavior in the temperature intervals of roughly 8–10 K and 10–30 K, respectively (Fig. 2).

At higher temperatures, the heat capacities of glassy rubbers could be approximated to by another scaling law, $C_p \sim T^\alpha$, with $\alpha \approx 0.9$. Empirically, the low value of the exponent α may be regarded as an indication of a cross-over to a high-temperature vibration regime with a dominant contribution of one-dimensional, intramolecular excitations to the total vibrational density of the states.

As could be expected, the absolute values of C_p and the slopes of the corresponding C_p vs. T plots for filled samples decreased, the higher the filler content (Fig. 1); however, a quantitative discussion of these trends as outlined above ought to be postponed until the low-temperature values of C_p for carbon black become available.

Glass transition region

As can be seen from Fig. 1 the glass-rubber transitions at $T_g = 202 \pm 2$ K (SKI-3) and 215 ± 2 K (SKMS-30) manifest themselves as sudden heat capacity jumps [$\Delta C_p(O) = 0.360 \pm 0.010$ J g⁻¹ K⁻¹ and 0.350 ± 0.010 J g⁻¹ K⁻¹, respectively]. Within the limits of experimental uncertainty, the values of T_g for filled and unfilled samples were the same; moreover, the apparent heat capacity jumps for filled samples, $\Delta C_p(\varphi)$, proved to be very close to the corresponding additive values, $\Delta C_p(O)(1-\varphi)$. Thus, it appears that the claim for the existence of BR (if any) in filled rubbers should be based on experimental evidence other than static heat capacity measurements in the relatively narrow temperature interval around the glass transition [6].

Thermodynamic quantities

Pragmatically, within the limits of experimental uncertainty, the raw values of C_p for all studied samples in the solid (glassy) state below T_g could be fitted to the 6-power polynomials of temperature (Table 2). These polynomials were subsequently used to derive the smoothed values of C_p in the temperature interval from 0 K to T_g ; at higher temperatures, the raw data were smoothed graphically on the assumption of a linear temperature dependence of C_p in the rubbery state. The smoothed values of C_p for carbon black below 80 K were calculated from the empirical relationship C_p [J kg⁻¹ K⁻¹] = $0.2195 T^{1.464}$, which

Table 2 Coefficients of the equation $C_p/\text{J kg}^{-1} \text{K}^{-1} = A + BT + CT^2 + DT^3 + ET^4 + FT^5 + GT^6$

| Sample | A | B | C×10 ² | D×10 ⁵ | E×10 ⁶ | F×10 ⁸ | G×10 ¹¹ |
|--------|--------|------|-------------------|-------------------|-------------------|-------------------|--------------------|
| M340 | -49.32 | 9.72 | -4.18 | -8.70 | 3.87 | -2.40 | 4.84 |
| M342 | -43.20 | 7.58 | -2.66 | -12.0 | 3.91 | -2.66 | 5.88 |
| M344 | -38.14 | 7.74 | -4.78 | 21.1 | 1.03 | -1.21 | 2.91 |
| D200 | -54.50 | 9.08 | -3.85 | -3.35 | 2.35 | -1.23 | 2.05 |
| D240 | -50.74 | 8.24 | -7.62 | 77.6 | -4.13 | 1.05 | -0.90 |

quantitatively fitted the raw data in the entire temperature interval 80–300 K (dotted line in Fig. 1).

The absolute enthalpy, $H-H_0=\int C_p dT$, the absolute entropy, $S-S_0=\int C_p d \ln T$, and the absolute Gibbs free energy, $G=(H-H_0)-T(S-S_0)$ (where H_0 and S_0 are

Table 3 Thermodynamic functions of M-340

| T/K | $C_p/J \text{ kg}^{-1} \text{ K}^{-1}$ | $H-H_0/J \text{ kg}^{-1}$ | $S-S_0/J \text{ kg}^{-1} \text{ K}^{-1}$ | $-G/J \text{ kg}^{-1}$ |
|-------|--|---------------------------|--|------------------------|
| 2 | 3.0 | 3.0 | 1.5 | 0 |
| 5 | 8.5 | 20.25 | 6.3 | 11.25 |
| 10 | 43.6 | 150.5 | 21.45 | 64.0 |
| 20 | 128.2 | 1009 | 75.3 | 496.5 |
| 30 | 204.9 | 2675 | 141.5 | 1570 |
| 40 | 274.6 | 5073 | 210.0 | 3327 |
| 50 | 338.6 | 8139 | 278.2 | 5770 |
| 60 | 398.1 | 11820 | 345.2 | 8890 |
| 70 | 454.4 | 16085 | 410.8 | 12675 |
| 80 | 508.2 | 20900 | 475.0 | 17105 |
| 90 | 560.6 | 26240 | 538.0 | 22175 |
| 100 | 611.9 | 32105 | 600.0 | 27865 |
| 110 | 662.4 | 38475 | 660.4 | 34170 |
| 120 | 712.1 | 45350 | 720.2 | 41075 |
| 130 | 761.0 | 52715 | 779.1 | 48570 |
| 140 | 809.0 | 60565 | 837.3 | 56655 |
| 150 | 856.0 | 68890 | 894.7 | 65320 |
| 160 | 902.3 | 77680 | 951.4 | 74550 |
| 170 | 948.8 | 86935 | 1007 | 84350 |
| 180 | 997.1 | 96665 | 1063 | 94700 |
| 190 | 1050 | 106900 | 1118 | 105610 |
| 200 | 1111 | 117705 | 1174 | 117070 |
| 210 | 1500 | 130760 | 1237 | 129090 |
| 220 | 1553 | 146030 | 1308 | 141820 |
| 230 | 1589 | 161740 | 1378 | 155255 |
| 240 | 1625 | 177815 | 1447 | 169380 |
| 250 | 1661 | 194245 | 1514 | 184190 |
| 260 | 1697 | 211035 | 1580 | 199660 |
| 270 | 1733 | 228180 | 1644 | 215780 |
| 280 | 1769 | 245690 | 1708 | 232540 |
| 290 | 1805 | 263555 | 1771 | 249940 |
| 300 | 1840 | 281780 | 1832 | 267955 |

the zero-temperature enthalpy and entropy of a disordered glass), were calculated from the smoothed values of C_p obtained in this fashion (Tables 3–8). Finally, the corresponding excess thermodynamic quantities, P_{ex} , were derived from the standard relationship.

Table 4 Thermodynamic functions of M-342

| T/K | $C_p/J\text{ kg}^{-1}\text{ K}^{-1}$ | $H-H_0/J\text{ kg}^{-1}$ | $S-S_0/J\text{ kg}^{-1}\text{ K}^{-1}$ | $-G/J\text{ kg}^{-1}$ |
|-------|--------------------------------------|--------------------------|--|-----------------------|
| 2 | 2.8 | 2.8 | 1.4 | 0 |
| 5 | 7.5 | 18.25 | 5.75 | 10.6 |
| 10 | 32.6 | 118.5 | 17.65 | 58.0 |
| 20 | 102.8 | 795.5 | 59.65 | 397.5 |
| 30 | 167.8 | 2149 | 113.3 | 1251 |
| 40 | 228.2 | 4129 | 169.8 | 2664 |
| 50 | 284.9 | 6694 | 226.8 | 4647 |
| 60 | 338.9 | 9813 | 283.6 | 7200 |
| 70 | 390.9 | 13460 | 339.7 | 10320 |
| 80 | 441.5 | 17625 | 395.2 | 13995 |
| 90 | 491.0 | 22290 | 450.1 | 18220 |
| 100 | 539.5 | 27440 | 504.4 | 23000 |
| 110 | 586.8 | 33070 | 558.0 | 28310 |
| 120 | 632.6 | 39170 | 611.0 | 34160 |
| 130 | 676.6 | 45715 | 663.4 | 40530 |
| 140 | 718.9 | 52690 | 715.1 | 47425 |
| 150 | 759.5 | 60085 | 766.1 | 54835 |
| 160 | 799.3 | 67880 | 816.4 | 62750 |
| 170 | 840.2 | 76075 | 866.1 | 71160 |
| 180 | 885.2 | 84700 | 915.4 | 80070 |
| 190 | 939.0 | 93820 | 964.7 | 89470 |
| 200 | 1008 | 103560 | 1014 | 99365 |
| 210 | 1320 | 115200 | 1071 | 109760 |
| 220 | 1378 | 128690 | 1134 | 120790 |
| 230 | 1414 | 142650 | 1196 | 132440 |
| 240 | 1450 | 156970 | 1257 | 144710 |
| 250 | 1486 | 171650 | 1317 | 157580 |
| 260 | 1522 | 186690 | 1376 | 171050 |
| 270 | 1558 | 202090 | 1434 | 185100 |
| 280 | 1595 | 217860 | 1491 | 199730 |
| 290 | 1631 | 233980 | 1548 | 214930 |
| 300 | 1667 | 250470 | 1604 | 230690 |

$$P = \varphi P_1 + (1 - \varphi) P_2 + P_{ex}$$

where subscripts 1 and 2 refer to filler and rubber, respectively.

The results obtained (Fig. 3) reveal that the thermodynamic stability of the elastomeric phases in all filled samples is invariably lower (i.e. $G_{ex} > 0$) than for

Table 5 Thermodynamic functions of M-344

| T/K | $C_p/J \text{ kg}^{-1} \text{ K}^{-1}$ | $H-H_0/J \text{ kg}^{-1}$ | $S-S_0/J \text{ kg}^{-1} \text{ K}^{-1}$ | $-G/J \text{ kg}^{-1}$ |
|-------|--|---------------------------|--|------------------------|
| 2 | 3.0 | 3.0 | 1.5 | 0 |
| 5 | 7.8 | 19.2 | 6.09 | 11.25 |
| 10 | 34.7 | 125.5 | 18.67 | 61.20 |
| 20 | 99.4 | 796.2 | 60.89 | 421.6 |
| 30 | 157.4 | 2080 | 112.0 | 1279 |
| 40 | 210.1 | 3918 | 164.5 | 2661 |
| 50 | 259.0 | 6263 | 216.6 | 4568 |
| 60 | 305.3 | 9085 | 268.0 | 6994 |
| 70 | 349.9 | 12360 | 318.4 | 9928 |
| 80 | 393.6 | 16080 | 368.0 | 13360 |
| 90 | 437.0 | 20230 | 416.9 | 17290 |
| 100 | 480.2 | 24820 | 465.2 | 21700 |
| 110 | 523.4 | 29835 | 513.0 | 26590 |
| 120 | 566.5 | 35285 | 560.4 | 31960 |
| 130 | 609.2 | 41165 | 607.4 | 37800 |
| 140 | 651.3 | 47465 | 654.1 | 44110 |
| 150 | 692.9 | 54190 | 700.4 | 50880 |
| 160 | 734.2 | 61320 | 746.5 | 58115 |
| 170 | 775.8 | 68870 | 792.2 | 65810 |
| 180 | 819.0 | 76850 | 837.8 | 73960 |
| 190 | 865.7 | 85270 | 883.3 | 82565 |
| 200 | 919.3 | 94195 | 929.1 | 91630 |
| 210 | 1200 | 104790 | 980.7 | 101150 |
| 220 | 1266 | 117120 | 1038 | 111240 |
| 230 | 1302 | 129960 | 1095 | 121910 |
| 240 | 1337 | 143150 | 1151 | 133140 |
| 250 | 1372 | 156695 | 1207 | 144930 |
| 260 | 1407 | 170590 | 1261 | 157270 |
| 270 | 1442 | 184840 | 1315 | 170150 |
| 280 | 1478 | 199440 | 1368 | 183570 |
| 290 | 1513 | 214390 | 1420 | 197510 |
| 300 | 1548 | 229695 | 1472 | 211975 |

the corresponding unfilled rubbers. The structural implications of this fundamental result are difficult to assess at the present stage; nevertheless, it seems completely consistent with the idea that the macromolecules of both rubbers in filled samples assume somewhat altered (presumably more extended) conformations favoring better intermolecular packing (hence, $H_{ex} < 0$) as compared

Table 6 Thermodynamic functions of D-200

| T/K | $C_p/J \text{ kg}^{-1} \text{ K}^{-1}$ | $H-H_o/J \text{ kg}^{-1}$ | $S-S_o/J \text{ kg}^{-1} \text{ K}^{-1}$ | $-G/J \text{ kg}^{-1}$ |
|-------|--|---------------------------|--|------------------------|
| 2 | 2.8 | 2.8 | 1.4 | 0 |
| 5 | 7.5 | 18.25 | 5.75 | 10.5 |
| 10 | 32.38 | 118.0 | 17.60 | 58.0 |
| 20 | 111.7 | 838.1 | 61.70 | 395.9 |
| 30 | 183.8 | 2315 | 120.2 | 1292 |
| 40 | 249.5 | 4482 | 182.1 | 2801 |
| 50 | 309.9 | 7279 | 244.2 | 4933 |
| 60 | 365.9 | 10660 | 305.7 | 7685 |
| 70 | 418.6 | 14580 | 366.1 | 11050 |
| 80 | 469.0 | 19020 | 425.3 | 15010 |
| 90 | 518.1 | 23955 | 483.4 | 19555 |
| 100 | 566.6 | 29380 | 540.5 | 24680 |
| 110 | 615.0 | 35285 | 596.8 | 30365 |
| 120 | 663.8 | 41680 | 652.4 | 36610 |
| 130 | 713.3 | 48565 | 707.5 | 43415 |
| 140 | 763.5 | 55950 | 762.2 | 50765 |
| 150 | 814.5 | 63840 | 816.7 | 58660 |
| 160 | 866.1 | 72240 | 870.9 | 67100 |
| 170 | 918.4 | 81165 | 924.9 | 76075 |
| 180 | 971.3 | 90615 | 978.9 | 85595 |
| 190 | 1025 | 100595 | 1033 | 95655 |
| 200 | 1080 | 111120 | 1087 | 106255 |
| 210 | 1180 | 122425 | 1142 | 117390 |
| 220 | 1560 | 136125 | 1206 | 129090 |
| 230 | 1577 | 151810 | 1275 | 141500 |
| 240 | 1619 | 167790 | 1343 | 154600 |
| 250 | 1660 | 184190 | 1410 | 168370 |
| 260 | 1702 | 201000 | 1476 | 182800 |
| 270 | 1743 | 218220 | 1541 | 197890 |
| 280 | 1785 | 235870 | 1605 | 213630 |
| 290 | 1826 | 253920 | 1669 | 230000 |
| 300 | 1868 | 272385 | 1731 | 247000 |

Table 7 Thermodynamic functions of D-240

| T/K | $C_p/J\text{ kg}^{-1}\text{ K}^{-1}$ | $H-H_0/J\text{ kg}^{-1}$ | $S-S_0/J\text{ kg}^{-1}\text{ K}^{-1}$ | $-G/J\text{ kg}^{-1}$ |
|-------|--------------------------------------|--------------------------|--|-----------------------|
| 2 | 2.0 | 2.0 | 1.0 | 0 |
| 5 | 5.9 | 13.85 | 4.27 | 7.5 |
| 10 | 24.8 | 90.6 | 13.42 | 43.6 |
| 20 | 89.2 | 660.6 | 48.12 | 301.8 |
| 30 | 145.8 | 1836 | 94.72 | 1006 |
| 40 | 197.2 | 3551 | 143.7 | 2196 |
| 50 | 245.3 | 5763 | 192.9 | 3879 |
| 60 | 291.5 | 8447 | 241.7 | 6053 |
| 70 | 336.6 | 11590 | 290.0 | 8713 |
| 80 | 381.4 | 15180 | 337.9 | 11850 |
| 90 | 426.2 | 19215 | 385.4 | 15470 |
| 100 | 471.0 | 23700 | 432.6 | 19560 |
| 110 | 516.0 | 28640 | 479.6 | 24125 |
| 120 | 561.0 | 34020 | 526.5 | 29155 |
| 130 | 606.2 | 39860 | 573.2 | 34650 |
| 140 | 651.4 | 46145 | 619.7 | 40620 |
| 150 | 696.8 | 52890 | 666.2 | 47050 |
| 160 | 742.8 | 60085 | 712.7 | 53940 |
| 170 | 789.7 | 67750 | 759.1 | 61300 |
| 180 | 838.2 | 75890 | 805.6 | 69125 |
| 190 | 889.3 | 84525 | 852.3 | 77410 |
| 200 | 944.0 | 93690 | 899.3 | 86170 |
| 210 | 1040 | 103610 | 947.7 | 95400 |
| 220 | 1280 | 115210 | 1002 | 105120 |
| 230 | 1351 | 128365 | 1060 | 115430 |
| 240 | 1385 | 142050 | 1118 | 126320 |
| 250 | 1420 | 156075 | 1175 | 137795 |
| 260 | 1454 | 170445 | 1232 | 149830 |
| 270 | 1489 | 185155 | 1287 | 162430 |
| 280 | 1523 | 200210 | 1342 | 175580 |
| 290 | 1557 | 215610 | 1396 | 189270 |
| 300 | 1592 | 231360 | 1450 | 203500 |

with their classical random coil shape in unfilled samples; however this new conformational state turns out to be intrinsically less stable ($G_{ex}>0$) due to the concomitant severe loss of intramolecular (conformational) entropy ($S_{ex}<0$).

In this context, the differences observed in the magnitude of the excess quantities for filled samples based on SKI-3 or on SKMS-30 become especially illuminating. In fact, the significantly larger values of $-H_{\text{ex}}$ and $-S_{\text{ex}}$ implying better lateral packing of extended chain fragments in the filled samples of the former may be regarded as a quite natural consequence of its stereoregular molecular

Table 8 Thermodynamic functions of carbon black

| T/K | $C_p/J \text{ kg}^{-1} \text{ K}^{-1}$ | $H-H_0/J \text{ kg}^{-1}$ | $S-S_0/J \text{ kg}^{-1} \text{ K}^{-1}$ | $-G/J \text{ kg}^{-1}$ |
|-------|--|---------------------------|--|------------------------|
| 2 | 1.0 | 1.0 | 0.5 | 0 |
| 5 | 2.3 | 5.95 | 1.94 | 3.75 |
| 10 | 6.4 | 27.7 | 4.69 | 19.2 |
| 20 | 17.7 | 148.2 | 12.32 | 98.1 |
| 30 | 32.0 | 396.7 | 22.07 | 265.5 |
| 40 | 48.7 | 800.2 | 33.49 | 539.6 |
| 50 | 67.5 | 1381 | 46.33 | 935.4 |
| 60 | 88.2 | 2160 | 60.43 | 1466 |
| 70 | 110.5 | 3153 | 75.67 | 2144 |
| 80 | 134.4 | 4378 | 91.97 | 2980 |
| 90 | 159.7 | 5848 | 109.2 | 3983 |
| 100 | 186.4 | 7579 | 127.4 | 5164 |
| 110 | 214.3 | 9582 | 146.5 | 6532 |
| 120 | 243.4 | 11870 | 166.4 | 8094 |
| 130 | 273.7 | 14460 | 187.0 | 9860 |
| 140 | 305.0 | 17350 | 208.5 | 11835 |
| 150 | 337.5 | 20560 | 230.6 | 14030 |
| 160 | 370.9 | 24105 | 253.4 | 16450 |
| 170 | 405.4 | 27990 | 277.0 | 19100 |
| 180 | 440.8 | 32220 | 301.1 | 21990 |
| 190 | 477.1 | 36810 | 325.9 | 25120 |
| 200 | 514.3 | 41765 | 351.3 | 28505 |
| 210 | 552.4 | 47100 | 377.4 | 32150 |
| 220 | 591.3 | 52815 | 403.9 | 36050 |
| 230 | 631.1 | 58930 | 431.1 | 40225 |
| 240 | 671.7 | 65440 | 458.8 | 44675 |
| 250 | 714.1 | 72370 | 487.1 | 49400 |
| 260 | 755.2 | 79720 | 515.9 | 54415 |
| 270 | 798.1 | 87485 | 545.2 | 59720 |
| 280 | 841.8 | 95680 | 575.0 | 65320 |
| 290 | 886.2 | 104320 | 605.3 | 71220 |
| 300 | 939.3 | 113450 | 636.3 | 77430 |

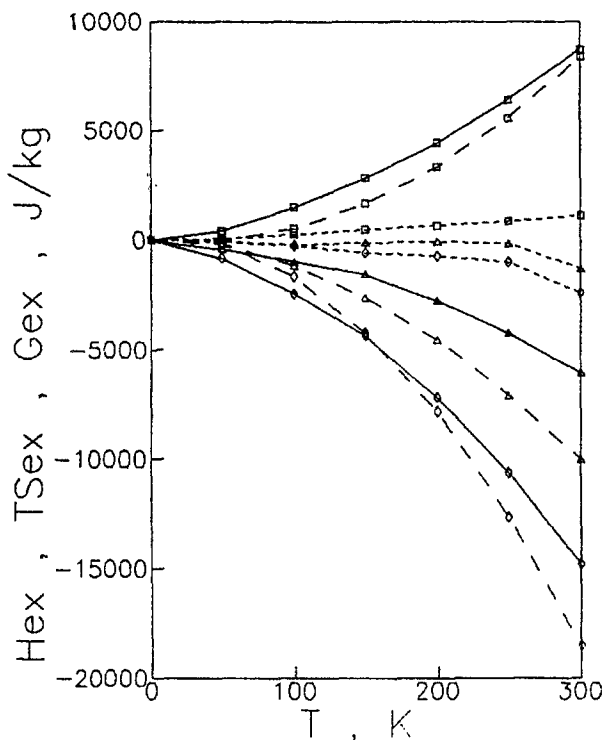


Fig. 3 Temperature dependence of H_{ex} (triangles), TS_{ex} (diamonds) and G_{ex} (squares) for M-342 (solid lines), M-344 (broken lines) and D-244 (dotted lines)

structure as contrasted with the irregular one of SKMS-30 [17]. Moreover, the trend to increases in $-H_{ex}$ and $-S_{ex}$ with filler content for SKI-3 (Fig. 3) is exactly that expected for a structural model of a filled rubber with BR distributed as shells of constant thickness around filler particles. According to a rough estimate, the apparent thickness of an elastomeric interlayer between filler particles in the highest-loaded sample M-344, $\langle L \rangle \cong 2r[(\varphi_M/\varphi)^{1/3}-1] \cong 15$ nm (assuming $2r \cong 30$ nm for the mean filler particle size and $\varphi_M \cong 0.8$ for the maximum packing fraction of polydisperse particles [6]), is comparable to the unperturbed radius of gyration of SKI-3 chains, $\langle R_g \rangle \cong 0.4 \langle h_0^2 \rangle^{1/2} \cong 11$ nm (assuming $\langle h^2 \rangle$ (nm²) $\cong 10^{-2} M$ [18] for the mean-square end-to-end distance and $M \cong 50 \times 10^3$ [17] for a typical molar mass of SKI-3 chains). In so far as $\langle R_g \rangle$ may be regarded as the minimum thickness of a polymer layer adsorbed on a solid surface [19, 20], the above estimates suggest that nearly all the elastomeric phase available in M-344 may exist as BR.

It is pertinent to note here that the value of $H_{ex} \cong -10$ J g⁻¹ for the latter sample at 300 K (Fig. 3) is very close in magnitude to the enthalpy difference between the equilibrium melt and the ideal crystal (i.e. the melting enthalpy) of *cis*-polyisoprene, $\Delta H_m^0 = 12.8$ J g⁻¹ [21]. In so far as H_{ex} is a measure of the en-

thalpy difference between the thermodynamic states of SKI-3 in filled and unfilled samples, respectively, it may be concluded that the former state is enthalpically equivalent to the crystalline state of SKI-3; as already emphasized, however, the overwhelming contribution of the unfavorable $S_{ex} < 0$ makes this filler-perturbed state intrinsically unstable ($G_{ex} > 0$).

Conclusions

1. Unfilled isoprene- and butadiene-methylstyrene-based rubbers behave essentially in a fracton-like way in the temperature interval 6–30 K.

2. Static heat capacity measurements in the glass transition interval are insufficient for a decision as to the existence of bound rubber in carbon black-filled rubbers.

3. The thermodynamic state of the elastomeric phase in carbon black-filled rubbers is intrinsically unstable.

References

- 1 G. Kraus, *Rubber Chem. Technol.*, **38** (1965) 1070.
- 2 B. B. Boonstra, *Polymer*, **20** (1979) 691.
- 3 S. Wolff and J.-B. Donnet, *Rubber Chem. Technol.*, **63** (1990) 32.
- 4 Yu. S. Lipatov, *Physical Chemistry of Filled Polymers*, Khimia, Moscow 1977 (in Russian).
- 5 P. S. Theocaris, *Adv. Polymer Sci.*, **66** (1985) 149.
- 6 V. P. Privalko and V. V. Novikov, *The Science of Heterogeneous Polymers: Structure and Thermophysical Properties*. Wiley, Chichester-New York Brisbane-Toronto-Singapore, 1995.
- 7 V. P. Azarenkov, A. V. Baibak, V. Yu. Kramarenko and V. P. Privalko, *Thermochim. Acta*, **238** (1994) 417.
- 8 W. H. Stockmayer and C. E. Hecht, *J. Chem. Phys.*, **21** (1953) 1954.
- 9 V. P. Azarenkov, A. V. Baibak, E. A. Kiryanova and V. P. Privalko, *Ukr. Polym. J.*, **2** (1993) 118.
- 10 V. K. Malinovsky, V. N. Novikov, A. P. Sokolov and V. A. Bagryansky, *Chem. Phys. Lett.*, **143** (1988) 111.
- 11 A. Blumen and H. Schnoerer, *Angew. Chemie*, **29** (1990) 113.
- 12 M. G. Zemlyanov, V. K. Malinovsky, V. N. Novikov, P. P. Parshin and A. P. Sokolov, *Zhurn. Eksp. Teoret. Fiz.*, **101** (1992) 284.
- 13 V. N. Novikov, A. P. Shebanin, V. P. Azarenkov, A. V. Baibak, V. Yu. Kramarenko and V. P. Privalko, *J. Raman Spectr.*, **25** (1994) 139.
- 14 S. Alexander and R. Orbach, *J. Phys.* **43** (1982) L625-L631.
- 15 S. Alexander, C. Laermans, R. Orbach and H. M. Rosenberg, *Phys. Rev.*, part B, **28** (1983) 4615.
- 16 J. P. Allen, *J. Chem. Phys.* **84** (1986) 4680.
- 17 N. V. Belozarov, *Rubber Technology*, Khimia, Moscow 1979 (in Russian).
- 18 A. E. Nesterov, *Properties of Polymer Solutions and Blends*-in 'Handbook on Physical Chemistry of Polymers', ed. by Yu. S. Lipatov, Vol. 1, Naukova Dumka, Kiev 1984 (in Russian).
- 19 G. I. Fleer and J. M. H. M. Scheutjens, *Adv. Colloid Interface Sci.*, **16** (1982) 341.
- 20 A. M. Skvortsov and A. A. Borbunov, *Vysokomol. Soed.*, ser. A, **28** (1986) 1941.
- 21 B. Wunderlich, *Macromolecular Physics*. Vol. 3: Crystal Melting, Academic Press, New York-London-Toronto-Sydney-San Francisco 1980.